Design of a Miniatured, Electromagnetic Quasi-Yagi Antenna with Circularly Polarized Characteristics

YunQi Zhang [1], LiFang Liu [1], Zhao Sun [2], XuPing Li [1], JunLing Che [3], and HaoYu Li[1]

[1]School of Electronic Engineering
Xi'an University of Posts & Telecommunications, Xi'an 710121, China
zhangyunqi@xupt.edu.cn, 1297629327@qq.com, lixuping@163.com, 779464178@qq.com

[2]Xi' an Branch
China Academy of Space Technology, Xi'an 710121, China
1050441091@qq.com

[3]School of Science
Xi'an University of Posts & Telecommunications, Xi'an 710121, China
junling.che@163.com

Abstract – A novel low-profile circularly polarized (CP) quasi-Yagi antenna with a wide 3-dB axial ratio (AR) bandwidth is proposed, which generates the endfire beam by combining magnetic microstrip cavity and folded electric dipoles with a $90°$ phase difference. The proposed antenna includes two shorting pins, which are employed to attain wider impedance bandwidth. Then, a phase delay line is added to connects two pairs of folded dipoles and a magnetic microstrip cavity to realize righthanded circularly polarized (RHCP). After optimization, a prototype with an overall size of $1.17 \times 0.91 \times 0.0387\lambda_0^3$ is designed. Simulated results demonstrate that the final model has 18.1% (5.01-6.01 GHz) 3-dB AR bandwidth and -10 dB impedance bandwidth of $5.2\%(5.67 - 5.97 \text{ GHz})$, respectively. In addition, experimental results demonstrate that the designed antenna is very applicable to the RFID system.

Index Terms – circularly polarized, endfire, folded dipoles, quasi-Yagi, RFID.

I. INTRODUCTION

Research on CP antennas can be traced back to the 1940s [1]. It can not only reduce the multipath effect, but also mitigate the polarization mismatch between receivers and transmitters [2–4]. Therefore, CP antennas are widely used in RFID systems [5], wireless communication [6] and satellite navigation receiving systems. Recently, endfire CP antennas have attracted much attention because of their two characteristics: strong directivity and high radiation efficiency. According to the difference in antenna structure, conventional endfire CP antennas can be roughly divided into two categories: helical antenna [7, 8] and Yagi-Uda antenna.

However, not all of them can realize the required performance, where the main beam is parallel to the antenna plane and the carrier can be invisible [9]. In [10], a typical planar endfire CP antenna is introduced, which is based on the combination of orthogonal magnetic dipole and the electric dipole. Nevertheless, the designed antenna exhibits exceptionally narrow impedance bandwidth and AR bandwidth (i.e., only 2.4% and 9.24% approximately). Recently, some efforts have been made to change this situation [11–16]. A wide impedance bandwidth has been explored through assembling magnetic dipoles and a V-shaped open loop in [11]. Reference [12] also demonstrates that a wide AR bandwidth can also be acquired by increasing electric dipole width. In [13], by using the concentric annular sector, a low-complexity antenna with wide AR bandwidth has been presented. So far, some novel CP endfire antennas are well-known for obtaining better radiation capacity. However, the gain is still relatively low as studied in [14–16].

Planar endfire CP quasi-Yagi antennas, carrying a parasitic strip in front of driven elements, are adopted to improve the antenna gain [17, 18]. Unsatisfactorily, most of the reported antennas may suffer from a deterioration in AR bandwidth or impedance bandwidth. In [19], a complex vertically polarized structure and horizontally polarized Yagi arrays are introduced to obtain good performance. Therefore, it is challenging and desirable to design a high gain, wide bandwidth planar endfire CP quasi-Yagi antenna.

A new complementary CP quasi-Yagi antenna is discussed in this communication. Two pairs of folded dipoles are used to expand the AR bandwidth, which are printed on the upper and lower layers of the dielectric substrate, respectively. A parasitic strip serves as the

director to improve the gain. The folded dipole and the magnetic microstrip cavity are connected by the phase delay line, and the 90° phase difference can be introduced by changing the length of the phase delay line. Finally, a CP quasi-Yagi antenna has been achieved, which generates a peak gain of 5.1 dBic. The designed antenna has approximately 4.3% measured impedance bandwidth and 14.1% AR bandwidth with an extremely low profile of $0.0387\ \lambda_0$.

II. ANTENNA DESIGN

The configuration of the proposed antenna with endfire CP characteristic is illustrated in Fig. 1, which is designed on a rectangular dielectric substrate F4B ($\tan\delta = 0.001$), a relative permittivity of $\varepsilon_r = 2.65$, and a thickness of $h = 2$ mm. As seen, the proposed antenna mainly comprises a magnetic microstrip cavity, phase delay line, director and two pairs of folded dipoles. The magnetic microstrip cavity, connecting with two pairs of folded dipoles by phase delay line, is composed of three short edges and an open aperture. In addition, two shorting pins are placed in the magnetic microstrip cavity to excite the disturbance field and broaden the impedance bandwidth [20]. The antenna has the same top and bottom layout. A coaxial connector with a characteristic impedance of 50 Ω in which the inner conductor is connected to the upper layer and the outer conductor is welded to the lower layer. The director is added in the endfire direction to enhance the gain and radiation efficiency. All actual dimensions of the proposed antenna are as follows: $L_1 = 60.5$ mm, $W_1 = 47.1$ mm, $L_2 = 14.25$ mm, $W_2 = 8.2$ mm, $L_3 = 5.4$ mm, $W_3 = 0.34$ mm, $L_4 = 9.9$ mm, $W_4 = 3.8$ mm, $L_5 = 7.6$ mm, $L_6 = 4$ mm, $L_7 = 7.6$ mm, $Lx = 12.1$ mm, $Wx = 2.1$ mm, $d = 0.3$ mm, $d_1 = 0.7$ mm, $g = 4.2$ mm, $W_5 = 3.2$ mm, $\alpha = 85°$.
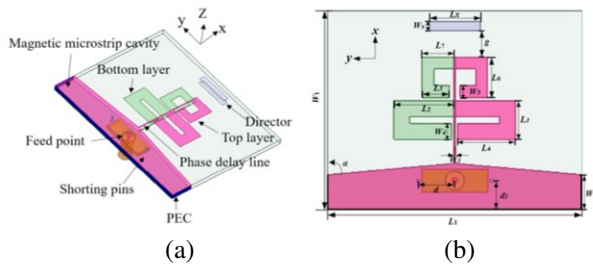
line. The 90° phase difference is mainly provided by the length d of the phase shift line between them, as shown in Fig. 2. Among them, the magnetic dipole produces an "eight" shaped radiation pattern in the azimuth plane (xoy-plane) and an "O" shaped radiation pattern in the elevation plane (xoz-plane). The result proves that the antenna resonates as a vertically polarized electromagnetic wave. The electric dipole has a complementary orthogonal mode with respect to the magnetic dipole.
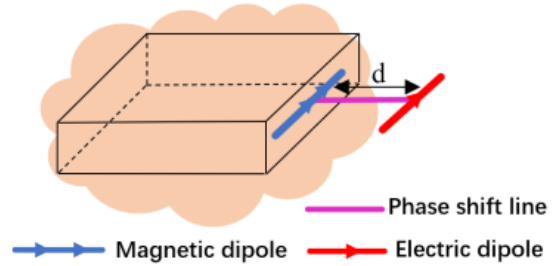
Fig. 2. Schematic diagram of the proposed antenna.

To clarify the design criteria of the proposed antenna, the design processes are present in Fig. 3 from ANT 1 to ANT 4 , and corresponding simulation results are displayed in Fig. 4. ANT 1 has an original printed electric dipole without shorting pins. In ANT 2, electric dipoles have been folded and two shorting pins are added based on ANT 1. As for ANT 3, an additional folded printed electric dipole is introduced compared with ANT 2. The final structure can be obtained by adding a director above ANT 3 .

By properly designing the antenna structure, the simulated $|S_{11}|$, AR and gain results of these antennas are presented in Fig. 4. First, by adding shorting pins and

A. Design procedure

The simple model of antenna is mainly composed of a magnetic dipole, electric dipole and phase delay

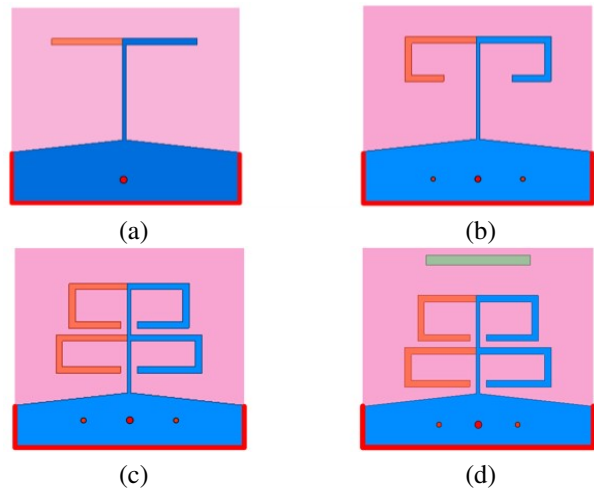Fig. 1. Geometry for the proposed antenna. (a) 3-D structure; (b) Top view.

Fig. 3. Evolution processes for the quasi-Yagi antenna. (a) ANT 1; (b) ANT 2; (c) ANT 3; (d) ANT 4.

folded dipoles, the axial ratio and reflection coefficient are greatly reduced (For ease of comparison, the same resonant frequency is used for each antenna). Second, it can be observed from Fig. 4 (b) that 3 dB AR bandwidth is greatly improved, and two resonance points appear at 5.4 GHz and 6.05 GHz by properly introducing a pair of folded dipoles. Finally, after adding the director, the gain of the designed antenna is up to 4.9 dBic.
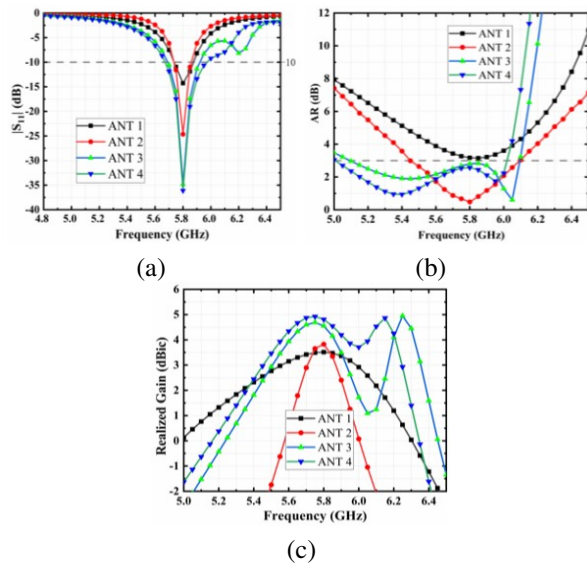

Fig. 4. Results of the process of the cp quasi-Yagi antenna. (a) $|S_{11}|$; (b) AR; (c) Realized gain.

B. Operating mechanism

A circular polarization wave could be generated with two electric field vectors of the same amplitude and $90°$ phase difference. The working principle of the proposed antenna is shown in Fig. 5, where Fig. 5 (a) refers to the equivalent model of the magnetic microstrip cavity [12]. The equivalent magnetic current source is parallel to the y-axis, the included angle between the x and y-axis is φ, and the included angle between y and z axis is θ. It can be known from the literature that the normalized electric field generated by the aperture at any point in free space in Fig. 5 (a) is:

$$\vec{E}_{\text{aperture}} = \vec{E}_{\theta} + \vec{E}_{\varphi} = \hat{\theta}\cos\varphi + \hat{\varphi}\cos\theta\sin\varphi. \quad (1)$$

Figure 5 (b) put forward an equivalent source model of two pairs of folded dipoles. To simplify the analysis and reveal the radiation characteristics of the folded dipole antenna, it is assumed that all equivalent current sources or current sheets are ideal short dipoles [11]. It can be seen from Fig. 5 (b) that the current components in the x-direction cancel each other, while the current

components in the y-direction are linearly superposed. Consequently, the main radiation characteristics of the folded dipole should be determined by the y-direction components of the eight current sheets. Therefore, we can get the normalized electric field intensity superimposed by the folded dipole vector as follows:

$$\vec{E}_{\text{dipole}} = \vec{E}_{\theta} + \vec{E}_{\varphi} = \hat{\theta}\cos\theta\sin\varphi + \hat{\varphi}\cos\varphi. \quad (2)$$

Figure 5 (c) shows the entire operating mechanism of the proposed antenna. The magnetic microstrip cavity and the folded dipoles are excited with equal amplitudes and $90°$ phase difference, and no additional time phase difference ($\delta_0 = 0$) is introduced. The total far-field of the combined geometry will be:

$$\vec{E}_{\text{total}} = \vec{E}_{\text{aperture}} + e^{-j(kd\sin\theta\cos\varphi+\delta_0)}\vec{E}_{\text{dipole}}. \quad (3)$$

By substituting equation (2) into equation (3), the normalized electric field in the x-direction ($\theta = 90°, \varphi = 0°$) can be obtained as:

$$\vec{E}_{+x} = \hat{\theta} + \hat{\varphi}j. \quad (4)$$

It can be seen from equation (4) that the amplitude is equal and the phase difference is $90°$ in the $+x$ direction, and the ideal circular polarization radiation characteristic can be obtained [21].
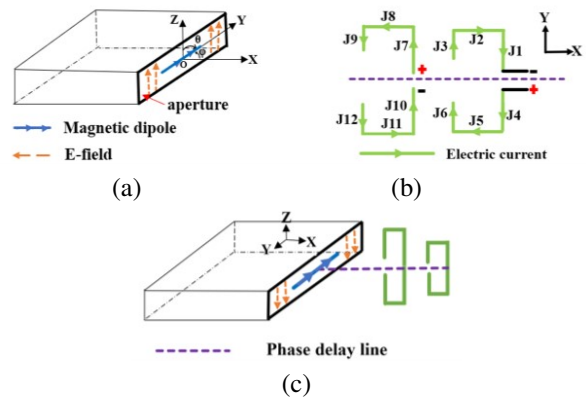

Fig. 5. Operating principle of this antenna. (a) Equivalent model of aperture element; (b) Equivalent source model of two-element folded dipole; (c) Working principle of the proposed antenna.

A $90°$ phase difference is necessary to generate circularly polarized waves. There are many ways to introduce a $90°$ phase difference, such as adding EZR-MZR resonances [22], dual-feed and phase delay line. However, it is mainly produced by adjusting the length of the phase delay line in this paper.

To further demonstrate the mechanism of the circular polarization radiation, the simulated vector surface current distributions of the short magnetic wall and director at different times $t = 0$, $T/4$, $T/2, 3\,T/4$ are exhibited from Figs. 6 (a) to (d) at 5.8 GHz, respectively. The director current can be obtained by coupling the current on the folded dipoles. Note that a solid red thick arrow in the upper right corner of each plot represents the synthetic short magnetic wall current and director current. By analyzing the trajectory of the synthetic current, the polarization mode of the proposed antenna can be clearly understood.

As demonstrated in Fig. 6 (a), the vector current of the short magnetic wall is toward the $+z$-axis, while the vector current of the director is toward the $+y$-axis. Therefore, the total current I_1 can be synthesized at $t = 0T$. As shown in Fig. 6 (b), the new vector total current (I_2) can be obtained at $t = T/4$ with the change of director current. According to the analysis, this change is mainly caused by the current change on the longer folded dipole. Regarding Fig. 6 (c), it is clearly shown that the synthetic current I_3 can be acquired due to the transformation of the current direction on the short magnetic wall. Similarly, I_4 can be attained with similar method. From the above description, it can be inferred that a clockwise polarization wave is formed on the yoz-plane. Utilizing the right-hand spiral criterion, it can be concluded that the antenna has realized the RHCP radiation in $+x$ direction.

C. Operating mechanism

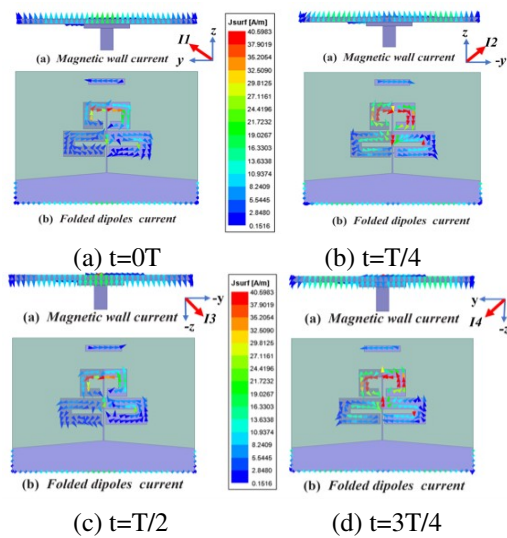The performance of the proposed antenna shows greater sensitivity for variation in some parameters, such as the length (L_1) and width (W_2) of the magnetic microstrip cavity. As depicted in Fig. 7 (a), L_1 has a significant impact on the AR of the designed antenna. With the increase of L_1, the magnetic dipole current component is strengthened, and the AR is well improved. However, when L_1 increases to a certain extent, the AR performance deteriorates because the vertical electric field component is larger than the horizontal electric field component and the amplitude is not equal. It can be seen that when L_1 is equal to 60.5 mm, the optimal results of AR performance can be obtained.

It can be seen from Fig. 7 (b) that W_2 has a significant effect on the resonant frequency of the designed antenna. With the change of W_2, the resonant frequency of the antenna is constant change. The change of W_2 is equivalent to the movement of the position of the coaxial feed point. When W_2 is selected as 8.2 mm, the resonant frequency works exactly at 5.8 GHz.

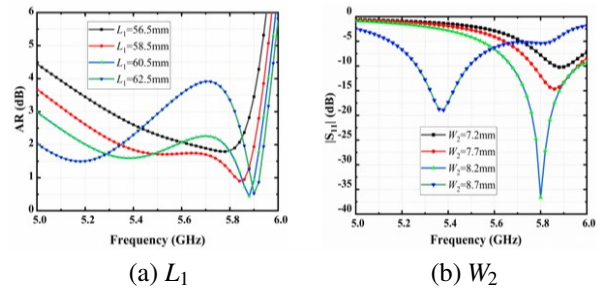Thereby, the designed antenna can be used in the RFID system.

(a) L_1 (b) W_2

Fig. 7. Parameter study of L_1 and W_2. (a) L_1. (b) W_2.

III. EXPERIMENTAL RESULTS

A prototype, as shown in Fig. 8, was made to verify the characteristic of the proposed antenna. The measured results of reflection coefficient are obtained with the Agilent network analyzer, while the radiation and AR results are obtained in the anechoic chamber, as depicted in Fig. 8 (a).

Following Fig. 9 (a), the curves of simulated and measured reflection coefficients present similar variation trends. However, some discrepancies and fluctuations exist between the measured and simulation results, mainly owing to the unavoidable test errors. Finally, the measured -10 dB bandwidth is from 5.7 to 5.95 GHz, a reduction of about 50 MHz concerning the simulation results ($5.67 - 5.97$ GHz).

The results of AR, gain are shown in Fig. 9 (b) and Fig. 9 (c), respectively. The simulation results with the measurement results of AR and realized gain are reasonably inconsistent, which may occur due to coaxial connector connection and fabrication errors. The
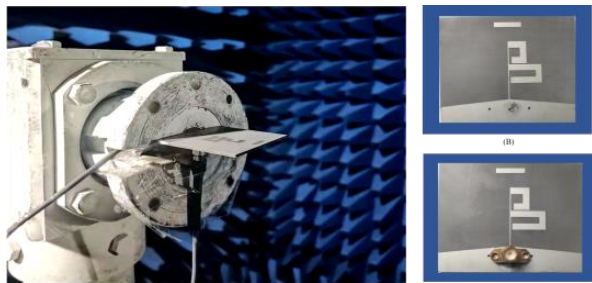

(a) t=0T   (b) t=T/4

(c) t=T/2   (d) t=3T/4

Fig. 6. The current distribution diagram is at 5.8 GHz. (a) t = 0 T; (b) t = 1/4 T; (c) t = 1/2 T; (d) t = 3/4T.

Fig. 8. (a) Measurement setup in the anechoic chamber. (b) The top view; (c) The back view.
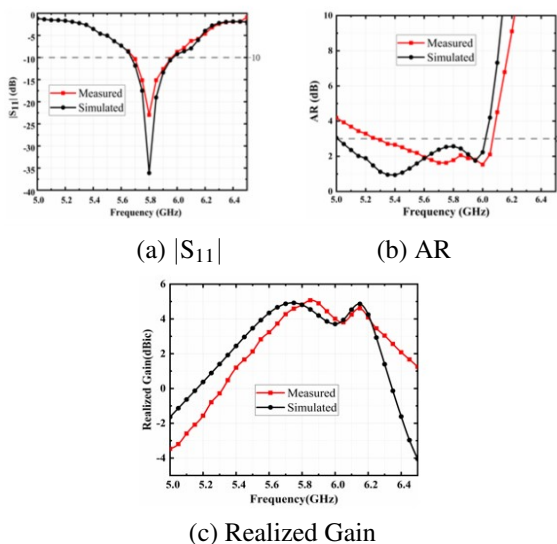

(a) $|S_{11}|$ (b) AR

(c) Realized Gain

Fig. 9. Simulated and measured result for the proposed antenna. (a) $|S_{11}|$; (b) AR; (c) Realized gain.

experimental results illustrate that the proposed antenna achieves bandwidths of $14.1\%(5.27-6.07\ \text{GHz})$ for AR < 3 dB and the gain can reach 5.1 dBic in the operating range. Although the experimental results of AR bandwidth and impedance bandwidth are narrow, they can still be used in RFID systems.
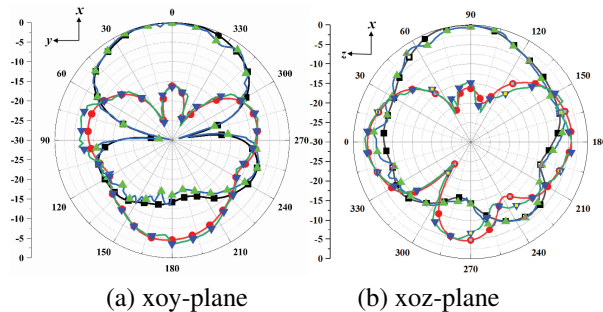

(a) xoy-plane   (b) xoz-plane

Fig. 10. Simulated and measured normalized radiation patterns at 5.8 GHz for the quasi-Yagi antenna.

The normalized radiation patterns of the two main radiation planes at 5.8 GHz are shown in Fig. 10. Obviously, this antenna has a unidirectional RHCP mode in the desired operating frequency band. In addition, Table 1 gives a comparison of this antenna with other endfire CP antennas to highlight its advantages. It can be seen that the designed antenna has an appropriate size, wider AR bandwidth and higher gain. Based on its planar structure and easy integration, it is suitable for some terminal devices.

Table 1: Comparison of various endfire *CP* antennas

Ref	BW/%	AR/%	Peck Gain (dBic)	Size $/\lambda_0^3$
10	2.4	9.2	2.6	$0.59 \times 0.73 \times 0.053$
12	1.9	14.5	2.3	$0.99 \times 0.87 \times 0.053$
15	4.3	4.3	3.3	$1.74 \times 0.72 \times 0.0387$
17	1	1.5	7.2	$1.05 \times 0.65 \times 0.026$
18	5.2	5	7.8	$1.74 \times 0.97 \times 0.0387$
Pro	4.3	14.1	5.1	$1.17 \times 0.911 \times 0.0387$

IV. CONCLUSION

In this letter, A circularly polarized quasi-Yagi antenna with wide AR bandwidth and high gain is designed. A circularly polarized beam is formed by a combination of two pairs of folded electric dipoles and magnetic dipoles. The folded dipoles are used as driving elements in this antenna to improve the AR bandwidth. Two shorting pins are used to improve antenna impedance matching. The simulation and actual measurement of the antenna proved that the center frequency of the antenna was 5.8 GHz, which covers the frequency range of the RFID systems well.

ACKNOWLEDGMENT

REFERENCES

[1] J. D. Kraus, "Helical beam antennas for wide-band applications," *Proc. IRE*, vol. 36 , no. 10 , pp. 1236-1242, 1948.

[2] Y. Cheng and Y. Dong, "Wideband circularly polarized split patch antenna loaded with suspended rods," *IEEE Antennas Wirel. Propag. Lett.*, vol. 20, no. 2, pp. 229-233, 2021.

[3] Q. Chen, H. Zhang, L.-C. Yang, B. Xue, and Y.-C. Zeng, "Compact microstrip-via-fed wideband circularly polarized antenna with monofilar, spiral

stub for C-band applications," *Int. J. RF Microwav. Comput-Aided Eng.*, vol. 27, no. 7, e21118, 2017.

[4] Y.-H. Yang, B.-H. Sun, and J.-L. Guo, "A sin-glelayer wideband circularly polarized antenna for millimeter-wave applications," *IEEE Trans. Antennas Propag.*, vol. 68 , no. 6 , pp. 4925-4929, 2019.

[5] Y. Pan and Y. Dong, "Circularly polarized stack Yagi RFID reader antenna," *IEEE Antennas Wirel. Propag. Lett.*, vol. 19, no. 7, pp. 1053-1057, 2020.

[6] T.-V. Hoang, T.-T. Le, Q.-Y. Li, and H.-C. Park, "Quad-band circularly polarized antenna for 2.4/5.3/5.8-GHz WLAN and 3.5-GHz WiMAX applications," *IEEE Antennas Wirel. Propag. Lett.*, vol. 15, pp. 1032-1035, 2016.

[7] X.-D. Bai, J. J. Tang, X.-L. Liang, J.-P. Geng, and R.-H. Jin. "Compact design of triple-band circularly polarized quadrifular helix antennas," *IEEE Antennas Wirel. Propag. Lett.*, vol. 13, pp. 380-383, 2014.

[8] C.-R. Liu, Y.-X. Guo, and S.-Q. Xiao, "Circularly polarized helical antenna for ISM-band ingestible-capeule endoscope systems," *IEEE Trans. Antennas Propag.*, vol. 62, no. 12 , pp. 6027-6039, 2014.

[9] J. Huang and A.-C. Densmore, "Microstrip Yagi array antenna for mobile satellite vehicle application," *IEEE Trans. Antennas Propag.*, vol. 39 , no. 7, pp. 1024-1030, 1991.

[10] W.-J. Lu, J.-W. Shi, K.-F. Tong, and H.-B. Zhu, "Planar endifre circularly polarized antenna using combined magnetic dipoles," *IEEE Antennas WJol Propag. Lett.*, vol. 14, pp. 1263-1266, 2015.

[11] M. You, W.-J. Lu, B. Xue, L. Zhu, and H.-B. Zhu, "A novel planar endfire circularly polarized antenna with wide axial-ratio beamwidth and wide impedance bandwidth," *IEEE Trans. Antennas Propag.*, vol. 64 , no. 10 , pp. 4554-4559, 2016.

[12] W.-H. Zhang, W.-J. Lu, and K. W. Tam, "A planar end-fire circularly polarized complementary antenna with beam in parallel with its plane," *IEEE Trans. Antennas Propag.*, vol. 64, no. 3, pp. 1146-1152, 2016.

[13] B. Xue, M. You, W.-J. Lu, and L. Zhu, "Planar end-fire circularly polarized antenna using concentric amnular sector complementary dipoles," *Int. J. RF Microwa. Comput.-aid. Eng*. vol. 26, no. 9, pp. 829-838, 2016.

[14] H.-Q. Yang, M. You, W.-J. Lu, L. Zhu, and H. Zhu, "Envisioning an endfire circularly polarized antenna: presenting a planar antenna with a wide beamwidth and enhanced front-to-back ratio," *IEEE Antennas Propag. Mag.*, vol. 60, no. 4, pp. 70-79, 2018.

[15] J.-H. Liu, Y.-X. Li, Z.-X. Liang, and Y.-L. Long, "A planar quasi-magnetic-electric circularly polarized

antenna," *IEEE Trans. Antennas Propag.*, vol. 64, no. 6, pp. 2108-2114, 2016.

[16] J. Zhang, W.-J. Lu, H. Zhu, L. Zhu, and L. Li, "Wideband dual-mode planar endfire antenna with circular polarisation," *Electron. Lett*, vol. 52, no. 12, pp. 1000-1001, 2016.

[17] M. Ye, X.-R. Li and Q.-X. Chu, "Planar end-fire circularly polarized antenna with unidirectional radiation," *in IEEE International Symposium on Antennas and Propagation & USVC/URSI National Radio Science Meeting*, San Diego, CA. USA, pp. 2313-2314, 2017.

[18] Y. Cheng and Y. D. Dong, "A directive circularly polarized planar Yagi array antenna," *in IEEE International Symposium on Antennas and Propagation and USNC-URSI Radio Science Meting, Atlanta*, GA, USA, pp. 1351-1352, 2019.

[19] W.-L. Zhou, J.-X. Liu, and Y. L. Long, "A broad-band and high-gain planar complementary Yagi array antenna with circular polarization," *IEEE Trans. Antennas Propag. Lett.*, vol. 65, no. 3, pp. 1446-1451, 2017.

[20] Y. Gao, Z.-H. Xue, W.-M. Li, and W. Ren, "Widebeam planar end-fire circularly polarized antenna based on SIW," *International Conference on Microwave and Millimeter Wave Technology (ICMM)*, Guangzhou, China, pp. 1-3, 2019.

[21] C. A Balanis, *Antenna Theory: Analysis and Design*, 3rd ed, Wiley, Hoboken, NJ, USA, 2005.

[22] L. Peng, K. Sun, X. Jiang, S.-M. Li, and C.-L. Buan, "EZR-MZR resonators for compact low-profile omni-directional circular-polarized antenna design," *IEEE Photonics J.*, vol. 9, no. 4, pp. 1-15, 2017.

YunQi Zhang was born in Baglow Inner Mongolia, China in 1986. He received the PhD. degree from Xidjag, University, Xi'an, China in 2015. He is currently working in the Xi'an University of Posts & Telecommunications. His research interests include GPS antenna, CP antenna, omnidirectional antenna and antenna array designs.

LiFang Liu was born in Gansu, China, in 1994. She received the BEng degree from Lanzhou University of Technology, Gansu, China in 2017. Currently, she is pursuing an MS degree in Electronic Information from Xi'an University of Posts & Telecommunications. Her current interests include electromagnetic fields and microwave technology.

Zhao Sun was born in Shanxi, China, in 1988. She is currently working in Xi'an Branch of China Academy of Space Technology. Her current interests include low-orbit constellation and data link research.

JunLing Che is received the PhD degree in Electronic Science and Technology from Xi'an Jizgtong University, Xi'an, China in 2017. He is currently working in the Xi'an University of Posts & Telecommunications.
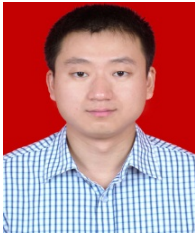
XuPing Li was born in Xi'an, Shanxi, China in 1981. He received the PhD. degree in Electromagnetic Field and Microwave from Xi'an University, Xi'an, China in 2015. In January 2019, he was transferred to Xi'an University of Posts and Telecommunications as the leader of the phased array antenna technology research team. The principal focus of his research program is the development of phased array antennas.

HaoYu Li was born in Anhui, China, in 1998. He received the BEng degree from Chyzhgu. University, Anhui, China in 2019. Currently, he is pursuing an MS degree in Electronic Information from Xi'an University of Posts & Telecommunications. His current interests include electromagnetic fields and microwave technology.